Received February 7, 2018, accepted March 25, 2018, date of publication March 29, 2018, date of current version April 25, 2018.

Digital Object Identifier 10.1109/ACCESS.2018.2820678

Theoretical Investigation of State Bistability Between Pure- and Mixed-Mode States in a 1550-nm VCSEL Under Parallel Optical Injection

DAN WANG[1], GUANG-QIONG XIA[1], YU-SHUANG HOU[1,2], WEN-YAN YANG[1,3], ELUMALAI JAYAPRASATH[1], JIAN-JUN CHEN[4], AND ZHENG-MAO WU[1]

[1]School of Physics, Southwest University, Chongqing 400715, China
[2]School of Science, Inner Mongolia University of Science and Technology, Baotou 014010, China
[3]School of Mathematics and Physics, Chongqing University of Science and Technology, Chongqing 400331, China
[4]School of Medical Engineering and Technology, Xinjiang Medical University, Urumqi 830011, China

Corresponding authors: Guang-Qiong Xia (gqxia@swu.edu.cn) and Zheng-Mao Wu (zmwu@swu.edu.cn)

This work was supported by the National Natural Science Foundation of China under Grant 61475127, Grant 61575163, and Grant 61775184.

ABSTRACT Based on the spin-flip model, state bistability (SB) between pure- and mixed-mode states in a 1550-nm vertical-cavity surface-emitting laser under parallel optical injection is theoretically investigated. The simulated results show that two types of SB can be observed when the injection light frequency (ν_{inj}) is smaller than the dominant mode frequency of the free-running laser (ν_e). For type-I SB, which occurs through fixing ν_{inj} and scanning injection power (P_{inj}) along different routes, there exist two hysteresis loops in which the laser operates at pure- or mixed-mode state, depending on the variation route of P_{inj}, and the hysteresis loop width increases sharply for increasing $|\Delta\nu|$ ($\Delta\nu = \nu_{\mathrm{inj}} - \nu_e$) with relatively strong P_{inj} whereas the loop width increases slowly for relatively weak P_{inj}, in agreement with our recent experimental report. Furthermore, type-II SB is also investigated through fixing P_{inj} and scanning ν_{inj} along different routes. There also exist two hysteresis loops in which the laser may operate at a pure- or mixed-mode state. With an increase of P_{inj}, the hysteresis loop width located at lower $|\Delta\nu|$ increases sharply and then decreases after reaching a maximum. However, for the hysteresis loop located at higher $|\Delta\nu|$, the loop width gradually increases with the increase of P_{inj}.

INDEX TERMS Vertical cavity surface emitting lasers, parallel optical injection, state bistability, hysteresis loop.

I. INTRODUCTION

Semiconductor lasers (SLs) subject to optical injection have received considerable attention in recent decades because of their fundamental characteristics and technological applications [1]–[19]. The injection-locking phenomenon of light is a special and stable dynamic characteristic and can be utilized to improve the performance of SLs via processes such as spectrum narrowing, modulation bandwidth enhancement, and frequency chirp reduction [1]–[3]. In addition, after introducing optical injection, SLs can be driven into various nonlinear dynamical states, such as period one, period two, quasi-period, and chaos, which have applications in the generation of photonic microwaves and fast physical random number, secure optical communication, chaotic lidar, *etc*. [9]–[20].

As a type of SL currently under development, vertical-cavity surface-emitting lasers (VCSELs) have received more attention because of their unique features, such as low threshold current, easy fabrication into two-dimensional arrays, high coupling efficiency to optical fibers, and low manufacturing cost [21]–[23]. Under different operating conditions, free-running VCSELs may oscillate at one of two orthogonal polarization modes; we refer to those modes as X and Y polarization modes. Therefore, depending on the relationship of the polarized direction between the injected light and the dominant mode in a solitary VCSEL, the optical injection can be categorized to orthogonal optical injection (OOI), variable polarization optical injection (VPOI) and parallel optical injection (POI). A considerable number of detailed theoretical and experimental investigations on

2169-3536 © 2018 IEEE. Translations and content mining are permitted for academic research only.
Personal use is also permitted, but republication/redistribution requires IEEE permission.
See http://www.ieee.org/publications_standards/publications/rights/index.html for more information.

the optical bistability in VCSELs subject to OOI and VPOI have been conducted [24]–[29]. For VCSELs under POI, most of the theoretical and experimental studies are focused on the injection locking (IL) and polarization switch (PS) phenomena [30]–[36]. Quirce *et al*. [32]–[34] have reported the frequency- and power-induced PS and IL in VCSELs under POI. Further, Denis-le Coarer *et al*. [35] experimentally and theoretically measured the mapping of the dynamic evolution of VCSELs under POI in parametric space of the injection power and frequency detuning. In addition, a special bistability phenomenon between IL along with PS (IL + PS) and solely injection locking (IL) have been observed in [32]–[36]. In principle, such bistability behavior can be classified as a state bistability (SB) between a mixed-mode state and a pure-mode state [37], [38]. Very recently, we have experimentally observed the performances of SB resulted by scanning injection power along different routes and analyzing the dependence of hysteresis loop width on the frequency detuning [38]. In this paper, based on the spin-flip model (SFM), we theoretically investigate the characteristics of such an SB (named type-I SB); the simulated results are in agreement with that reported in [38] after excluding the influence of the reflected injection light by the laser surface. In addition, the characteristics of another SB (named type-II SB) induced by scanning the frequency are also discussed.

II. THEORY

Based on the spin-flip model (SFM) [21], [39], the modified rate equations for a 1550-nm VCSEL under optical injection are as follows:

$$\frac{dE_x}{dt} = k(1+i\alpha)[(N-1)E_x + inE_y] - (\gamma_a + i\gamma_p)E_x + k_1 E_{inj,x} e^{i2\pi(\nu_{inj,x}-\nu_0)t} + \sqrt{\frac{\beta_{sp}}{2}}(\sqrt{(N+n)}\xi_+(t) + \sqrt{(N-n)}\xi_-(t)) \quad (1)$$

$$\frac{dE_y}{dt} = k(1+i\alpha)[(N-1)E_y - inE_x] + (\gamma_a + i\gamma_p)E_y + k_2 E_{inj,y} e^{i2\pi(\nu_{inj,y}-\nu_0)t} - i\sqrt{\frac{\beta_{sp}}{2}}(\sqrt{(N+n)}\xi_+(t) - \sqrt{(N-n)}\xi_-(t)) \quad (2)$$

$$\frac{dN}{dt} = \gamma_e[\mu - N(1+|E_x|^2+|E_y|^2]) - in(E_y E_x^* - E_x E_y^*) \quad (3)$$

$$\frac{dn}{dt} = -\gamma_s n - \gamma_e[n(|E_x|^2+|E_y|^2) + iN(E_y E_x^* - E_x E_y^*)] \quad (4)$$

where subscripts x and y represent the X and Y polarizations, respectively. E accounts for the slowly varying complex amplitude of the field. N corresponds to the total carrier population difference between the conduction and valence bands, and n denotes the difference between the carrier inversions for the spin-up and the spin-down radiation channels. k is the field decay rate, and α corresponds to the linewidth enhancement factor. γ_e is the decay rate of N, and γ_a and γ_p are the linear anisotropies representing dichroism and birefringence, respectively. γ_s is the spin-flip rate, and μ is the normalized bias current. k_1 and k_2 are the injection coefficients. E_{inj} is the amplitude of injection field, and $P_{inj} = |E_{inj}|^2$ is the injection power. β_{sp} is the spontaneous emission noise intensity. ξ_+ and ξ_- are Gaussian white noise terms of zero mean value. ν_{inj} is the frequency of injected light, and $\nu_0 = (\nu_x + \nu_y)/2$ is the intermediate frequency between the oscillation frequencies of X (ν_x) and Y (ν_y) polarizations. $\nu_x = \nu_0 + (\alpha\gamma_a - \gamma_p)/(2\pi)$, and $\nu_y = \nu_0 + (\gamma_p - \alpha\gamma_a)/(2\pi)$. For parallel optical injection (POI), the polarization direction of injection light is along the dominant mode of the solitary 1550-nm VCSEL. For convenience, in the following discussion, frequency detuning $\Delta\nu$ is defined as $\Delta\nu = \nu_{inj} - \nu_e$, where ν_e denotes the lasing frequency of the dominant mode in the solitary 1550-nm VCSEL.

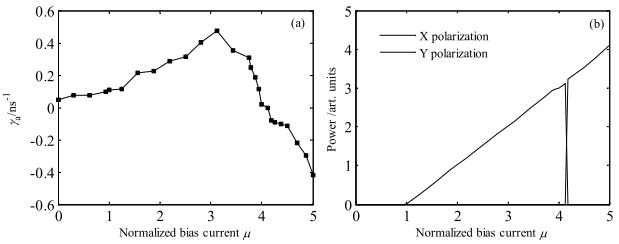

FIGURE 1. (a) Linear dichroism as a function of μ, and (b) polarization-resolved P-μ curve for a 1550-nm VCSEL operating in free-running mode.

III. RESULTS AND DISCUSSION

We numerically solved the rate equations (1)-(4) by the adopting fourth-order Runge-Kutta algorithm. In our simulation, we evaluated some parameters from [40]; these parameters are set as follows: $k = k_1 = k_2 = 33\ \text{ns}^{-1}$, $\gamma_s = 2100\ \text{ns}^{-1}$, $\gamma_e = 2.08\ \text{ns}^{-1}$. To make the simulated results match with our previous experimental results [38], the remaining parameters were suitably modified as follows: $\gamma_p = 110\ \text{ns}^{-1}$, $\alpha = 6.8$, and $\beta_{sp} = 10^{-6}\ \text{ns}^{-1}$. As demonstrated in [40], the value of γ_a depends on the normalized bias current μ. For fitting our experimentally measured polarization-resolved P-μ curve [38] together with taking into account the varied trend of γ_a with μ reported in [40], the used values of γ_a under different μ are given in Fig. 1(a). Under this condition, the polarization-resolved P-μ curve for the solitary 1550-nm VCSEL is simulated as shown in Fig. 1(b), which is consistent with our experimental result [38]. For $1 < \mu < 4.13$, the Y polarization is the dominant mode, whereas the X polarization is suppressed. When μ increases to 4.13, a sudden polarization switching (PS) from Y polarization to orthogonal X polarization is observed, and the current required for PS is identified as μ_{PS}. Further increasing the bias current to 5.00, the orthogonal X polarization mode plays the role of the dominant mode, whereas Y polarization is suppressed, and no further PS occurs. In the following discussion, to be consistent with

our previous experimental report [38], we consider two normalized bias currents of $\mu = 4.50$ and $\mu = 3.75$ for the discussion. For $\mu = 4.50$, the dominant mode is the X polarization mode; thus, only the X polarization mode is subjected to optical injection with injection power $P_{\text{inj}} = |E_{\text{inj,x}}|^2$ and frequency detuning $\Delta\nu = \nu_{\text{inj,x}} - \nu_{\text{x}}$ for POI. In contrast, for $\mu = 3.75$, the dominant mode switches to the Y polarization mode. Under this case, for POI, only the Y polarization mode is subjected to optical injection with injection power $P_{\text{inj}} = |E_{\text{inj,y}}|^2$ and frequency detuning $\Delta\nu = \nu_{\text{inj,y}} - \nu_{\text{y}}$.

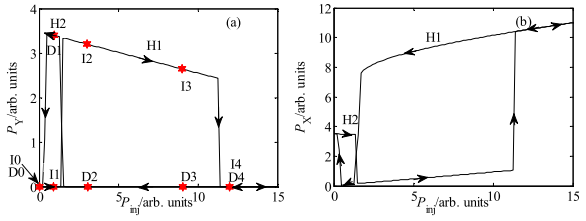

FIGURE 2. Output power as a function of the increase (solid lines) and decrease (dotted lines) of injection power under $\mu = 4.50$ and $\Delta\nu = -17.0$ GHz. (a) and (b) correspond to Y and X polarizations, respectively.

The injection parameters consist of the injection power P_{inj} and the frequency detuning $\Delta\nu$ ($=\nu_{\text{inj}} - \nu_{\text{e}}$) for parallel optical injection (POI). First, we discuss a type-I SB induced by scanning P_{inj} along different routes for a given $\Delta\nu$. Here, P_{inj} is gradually increased and decreased within a range 0-20.00 with a step of 0.15, and the time for P_{inj} stays on each step is 1 μs. Under $\mu = 4.50$ ($>\mu_{\text{PS}}$) and $\Delta\nu = -17.0$ GHz, the output power for the Y polarization (P_{Y}) and X polarization (P_{X}) with an increase (solid line) and decrease (dashed line) of P_{inj} are given in Fig. 2(a) and Fig. 2(b), respectively. As is evident from Fig. 2(a), the Y polarization mode is completely suppressed for a relatively small P_{inj}. Furthermore, the Y polarization oscillates when P_{inj} is increased to 1.35 and its output power is suddenly enhanced to 3.33; subsequently, P_{Y} presents a slowly decreasing trend for further increase of P_{inj}, which has been analyzed in [34]. When P_{inj} increases to 11.40, another abrupt change of P_{Y} is observed whereas the Y polarization mode is suppressed again. Further increasing P_{inj} to 20.00, the Y polarization remains in the switch-off state. However, during the gradual decrement process of P_{inj}, the Y polarization is not excited until P_{inj} is 1.50. When further decreasing P_{inj} to approximately 0.15, the Y polarization returns to the switch-off state again. As a result, depending on the varying routes of P_{inj}, the Y polarization mode is possibly excited for $0.15 < P_{\text{inj}} < 1.35$ and $1.50 < P_{\text{inj}} < 11.40$. The variation trend of the X polarization mode is shown in Fig. 2(b): the X polarization is never in the switch-off state. Therefore, SB between pure (sole X polarization) and mixed (X polarization + Y polarization) modes emerges through scanning P_{inj} along different routes. The hysteresis loops locating at higher- and lower-P_{inj} regions are represented as H1 and H2, respectively, where H1 corresponds to SB between injection locked X polarization and mixed-mode state and H2 corresponds to SB between period one X polarization and mixed-mode state. Compared with Fig. 3 in [38], the variation trend of Y polarization is identical; however, the simulated result for X polarization differs from the experimentally observed. The reason for this difference is that the experimentally measured output power of the X polarization contains a part of injected light reflected by the laser surface.

To reveal the physical mechanism of SB, Fig. 3 shows the optical spectra for increasing (a0-a4) or decreasing (b0-b4) P_{inj} for a few fixed values. Here, Figs. 3(a0-a4) and (b0-b4) correspond to points (I0-I4) and points (D0-D4) in Fig. 2(a), respectively. P_{X} is approximately 40 dB greater than P_{Y} without optical injection (Fig. 3(a0)), the X polarization is excited, and the Y polarization is suppressed. For the value of P_{inj} increasing to 0.90 (Fig. 3(a1)), the regenerated amplification of the injection light leads to a tiny decrease of P_{X}, which in turn results in the slight increase of P_{Y} via the carrier sharing mechanism between the X and Y polarizations. However, P_{Y} is still 40 dB smaller than P_{X}; thus, the Y polarization is unexcited. The spectral line locating at zero frequency offset originates from the four-wave mixing of the injected signal with the X polarization. When P_{inj} increases to 3.00 (Fig. 3(a2)), the X polarization is locked by the injection light. Under this case, the frequency offset to the central frequency ν_0 for X polarization is larger than that for Y polarization. As a consequence, the Y polarization acquires larger gain than the X polarization and translates into the dominant mode. Under this scenario, the laser operates in the mixed-mode (X polarization + Y polarization) state. Further increasing P_{inj} to 9.00 (Fig. 3(a3)), the similar optical spectrum with Fig. 3(a2) is observed, except for a smaller power difference between the two polarizations. As P_{inj} increases to 12.00 (Fig. 3(a4)), the Y polarization is completely suppressed, and only X polarization exists in the laser. However, when P_{inj} decreases from 20.00 to 12.00, 9.00, and 3.00, the 1550-nm VCSEL under POI remains the sole X polarization mode. The Y polarization is excited again for the value of P_{inj} decreases to 0.90 and the laser operates at the mixed-mode state. When P_{inj} decreases to 0, the X polarization is excited and the Y polarization is concealed again. Hence, the type-I SB phenomena occurred within the prescribed ranges of P_{inj}, as shown in Fig. 2. The type-I SB phenomena for the values of 0.90, 3.00, and 9.00 are shown in Fig. 3. Additionally, some spectral lines have a finite width, which is resulted by Gaussian white noise included in rate equations.

In our previous experimental report [38], we discussed the SB phenomenon that was observed under the condition of $\Delta\nu < 0$. Recently, the related investigations demonstrate that SB phenomenon can also be observed under $\Delta\nu > 0$ [35], [36]. In this work, we take the case of $\Delta\nu < 0$ as an example to discuss the SB characteristics. For different values of $\Delta\nu$, SB characteristics are different, as shown in Figs. 4(a1)-(a3). For a larger $|\Delta\nu|$, the hysteresis loop is wider for H1, but there was no noticeable change for H2, and the

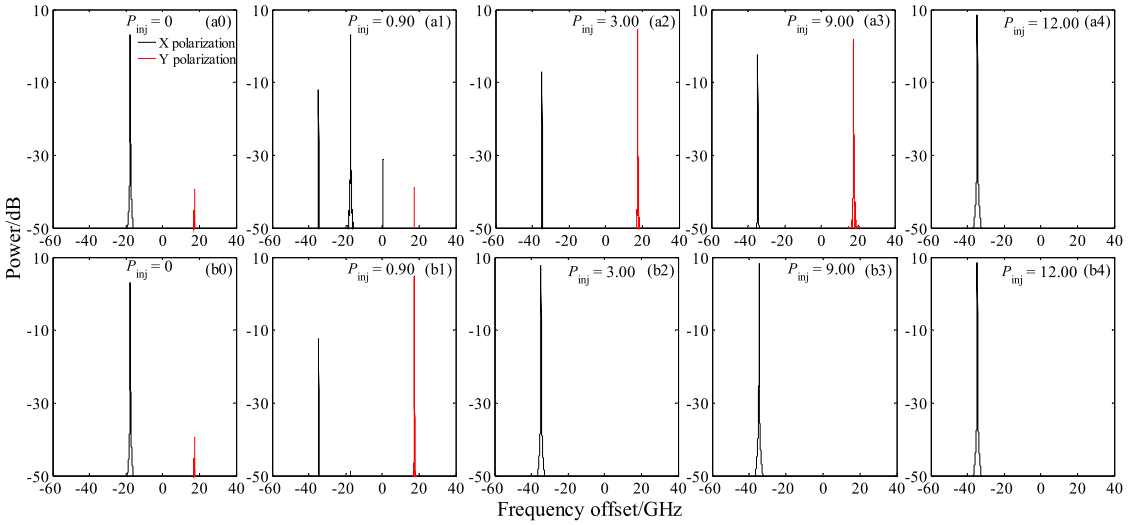

FIGURE 3. Simulated optical spectra of a 1550-nm VCSEL under POI with $\Delta\nu = -17.0$ GHz and different P_{inj}. The first, second, third, fourth, and fifth column represents $P_{inj} = 0$, 0.90, 3.00, 9.00 and 12.00, respectively. The first row represents the corresponding spectra of points (I0-I4) in Fig. 2(a), and the second row represents the corresponding spectra of points (D0-D4) in Fig. 2(a). The biased current is $\mu = 4.50$.

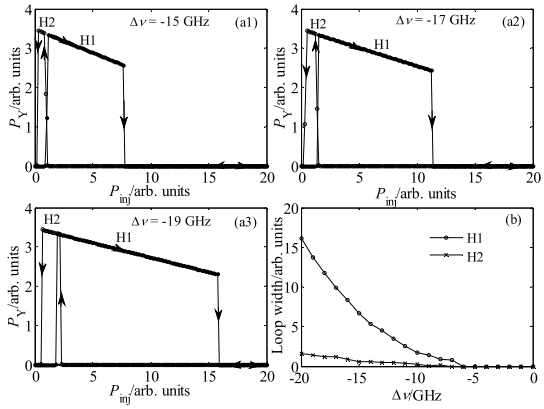

FIGURE 4. For $\mu = 4.50$ and different $\Delta\nu$, the dependence of output power on P_{inj} (a1)-(a3) and the H1 and H2 hysteresis loop widths as a function of $\Delta\nu$. Solid lines and dashed lines in (a1-a3) are for the cases of increasing P_{inj} and decreasing P_{inj}, respectively.

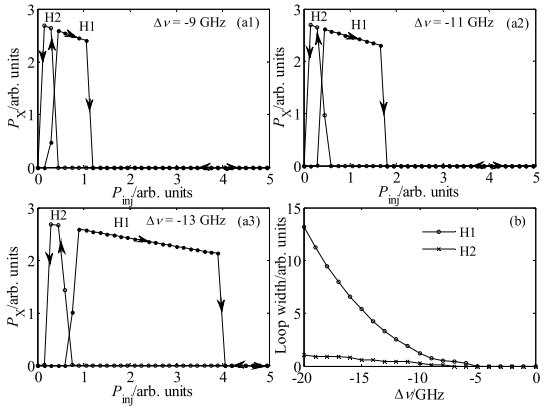

FIGURE 5. For $\mu = 3.75$ and different $\Delta\nu$, the dependence of the output power on P_{inj} (a1)-(a3) and H1 and H2 hysteresis loop widths as a function of $\Delta\nu$. Solid lines and dashed lines in (a1-a3) are for the cases of increasing P_{inj} and decreasing P_{inj}, respectively.

variations of the hysteresis loop width with $\Delta\nu$ are shown in Fig. 4(b). Obviously, the hysteresis loop width is increased quickly for H1 but is increased slowly for H2 with an increase of $|\Delta\nu|$ from 5 GHz. The variation trend for H1 and H2 is the same as the experimental results reported in [38].

The above results are obtained under $\mu = 4.50$, which is greater than PS current μ_{PS}. Next, we take $\mu = 3.75$ as an example to discuss SB characteristics for the case of $\mu < \mu_{PS}$; the obtained results are shown in Fig. 5. Note that, for the free-running 1550-nm VCSEL, the dominant mode switches to Y polarization; this phenomenon is different from the case of $\mu = 4.50$, and therefore the frequency detuning is $\Delta\nu = \nu_{inj,y} - \nu_y$ for POI. Figs. 5(a1)-(a3) show that there still exist two bistability hysteresis loops by scanning P_{inj} along different routes. Fig. 5(b) displays two hysteresis loop width variations with frequency detuning; the results are similar with that shown in Fig. 4(b). However, the width of H1 for $\mu = 3.75$ is smaller than that for $\mu = 4.50$ under the same value of $\Delta\nu$.

In [38], we experimentally investigated the type-I SB that is induced by scanning injection power P_{inj}, and the above discussed simulated results are in agreement with the reported experimental results. Additionally, as reported in [32], for a fixed value of $\Delta\nu$, the output spectrum of a 1550-nm VCSEL under POI is critically dependent on the process of varying $\Delta\nu$. As a result, type-II SB can be induced by scanning $\Delta\nu$ along different routes with a step of 1 GHz, and the time for $\Delta\nu$ stays at every step is 1 μs. Next, we discuss the performances of type-II SB. For a 1550-nm VCSEL biased at $\mu = 4.50$ under POI with $P_{inj} = 50.00$, through continuously

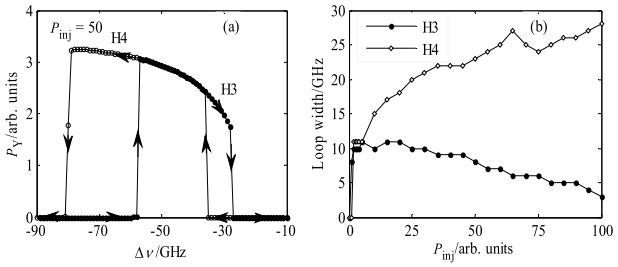

FIGURE 6. For $\mu = 4.50$, (a) output power as a function of frequency detuning under $P_{inj} = 50.00$, and (b) variation of hysteresis loop widths for H3 and H4 with P_{inj}. Solid lines and dashed lines in (a) are for the cases of increasing $\Delta\nu$ and decreasing $\Delta\nu$, respectively.

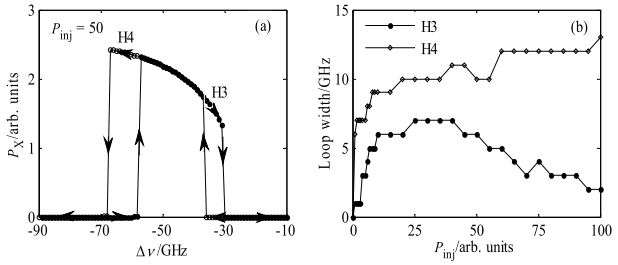

FIGURE 7. For $\mu = 3.75$, (a) output power as a function of frequency detuning under $P_{inj} = 50.00$, and (b) variation of hysteresis loop widths for H3 and H4 with P_{inj}. Solid lines and dashed lines in (a) are for the cases of increasing $\Delta\nu$ and decreasing $\Delta\nu$, respectively.

increasing (solid line) and decreasing (dashed line) frequency detuning $\Delta\nu$ ($=\nu_{inj,x} - \nu_x$), the variation curves of P_Y are shown in Fig. 6(a). Similar to the results of scanning P_{inj}, the X polarization is always excited and the Y polarization might be excited or not. There still exist two hysteresis loops; the hysteresis loops located at lower- and higher-$|\Delta\nu|$ regions are named H3 and H4, respectively, for convenience. The hysteresis loop width for H3 and H4 as a function of injection power P_{inj} is illustrated in Fig. 6(b). As shown in this diagram, the width of H3 and H4 initially increases sharply and then H3 decreases gradually whereas H4 increases continuously with an increase of P_{inj}. We repeat the type-II SB induced by scanning $\Delta\nu$ for different routes for $\mu = 3.75$; the results are shown in Fig. 7. Note that there still exist two hysteresis loops whose widths are smaller than those obtained under $\mu = 4.50$, and the variation trend of hysteresis loop widths with P_{inj} is similar with that obtained under $\mu = 4.50$.

IV. CONCLUSION

We reported in this paper the theoretical analysis of the state bistability (SB) between pure- and mixed-mode states in a 1550-nm VCSEL under parallel optical injection (POI), for which the polarization direction of the injection light is identical to that of the dominant mode in the free-running 1550-nm VCSEL. Initially, we showed the simulated characteristics of type-I SB are induced by scanning injection power P_{inj} in a 1550-nm VCSEL biased at $\mu = 4.50$ and $\mu = 3.75$, in accordance with the condition of our previous experimental result. The results showed that there exist two hysteresis loops in which the suppressed mode of the free-running laser is excited or not by POI, depending on the scanned route of P_{inj}. The hysteresis loop located at the region with relatively large P_{inj} is named H1, and the other is named H2. The width increases radically for H1 but slowly for H2 with an increase of $|\Delta\nu|$ ($\Delta\nu = \nu_{inj} - \nu_e$, ν_{inj} and ν_e are the frequency of the injected light and the dominant mode of the free-running laser, respectively). We confirmed that the hysteresis loop is wider when the bias current is large. All the characteristics obtained from the results are in good agreement with our previous experimentally observed results when we exclude the influence of the reflected injection light by the laser surface. Furthermore, we also discussed the performances of the type-II SB induced by scanning $\Delta\nu$ along different routes.

REFERENCES

[1] P. Gallion, H. Nakajima, G. Debarge, and C. Chabran, "Contribution of spontaneous emission to the linewidth of an injection-locked semiconductor laser," *Electron. Lett.*, vol. 21, no. 14, pp. 626–628, Jul. 1985.

[2] J. M. Liu, H. F. Chen, X. J. Meng, and T. B. Simpson, "Modulation bandwidth, noise, and stability of a semiconductor laser subject to strong injection locking," *IEEE Photon. Technol. Lett.*, vol. 9, no. 10, pp. 1325–1327, Oct. 1997.

[3] N. A. Olsson *et al.*, "Chirp-free transmission over 82.5 km of single mode fibers at 2 Gbit/s with injection locked DFB semiconductor lasers," *J. Lightw. Technol.*, vol. LT-3, no. 1, pp. 63–67, Feb. 1985.

[4] Z. G. Pan, S. Jiang, and M. Dagenais, "Optical injection induced polarization bistability in vertical-cavity surface-emitting lasers," *Appl. Phys. Lett.*, vol. 63, no. 22, pp. 2999–3001, Nov. 1993.

[5] G. H. M. van Tartwijk and D. Lenstra, "Semiconductor lasers with optical injection and feedback," *Quantum Semiclassical Opt.*, vol. 7, no. 2, pp. 87–143, Apr. 1995.

[6] M. Sciamanna and K. Panajotov, "Route to polarization switching induced by optical injection in vertical-cavity surface-emitting lasers," *Phys. Rev. A, Gen. Phys.*, vol. 73, no. 2, pp. 023811-1–023811-17, Feb. 2006.

[7] D. Zhong, Y. Ji, and W. Luo, "Controllable optoelectric composite logic gates based on the polarization switching in an optically injected VCSEL," *Opt. Exp.*, vol. 23, no. 23, pp. 29823–29833, Nov. 2015.

[8] B. Jiang *et al.*, "Polarization switching characteristics of 1550-nm vertical-cavity surface-emitting lasers subject to double polarization pulsed injection," *IEEE J. Quantum Electron.*, vol. 52, no. 11, Nov. 2016, Art. no. 2400707.

[9] T. B. Simpson, J. M. Liu, K. F. Huang, and K. Tai, "Nonlinear dynamics induced by external optical injection in semiconductor lasers," *Quantum Semiclass. Opt., J. Eur. Opt. Soc. B*, vol. 9, no. 5, pp. 765–784, May 1997.

[10] S. K. Hwang and J. M. Liu, "Dynamical characteristics of an optically injected semiconductor laser," *Opt. Commun.*, vol. 183, nos. 1–4, pp. 195–205, Sep. 2000.

[11] W.-Q. Zhu *et al.*, "Dynamics of a monolithically integrated semiconductor laser under optical injection," *IEEE Photon. Technol. Lett.*, vol. 27, no. 20, pp. 2119–2122, Oct. 15, 2015.

[12] J. J. Chen *et al.*, "Generation of polarization-resolved wideband unpredictability-enhanced chaotic signals based on vertical-cavity surface-emitting lasers subject to chaotic optical injection," *Opt. Exp.*, vol. 23, no. 6, pp. 7173–7183, Mar. 2015.

[13] S.-C. Chan, S.-K. Hwang, and J.-M. Liu, "Period-one oscillation for photonic microwave transmission using an optically injected semiconductor laser," *Opt. Exp.*, vol. 15, no. 22, pp. 14921–14935, Oct. 2007.

[14] S.-C. Chan and J.-M. Liu, "Microwave frequency division and multiplication using an optically injected semiconductor laser," *IEEE J. Quantum Electron.*, vol. 41, no. 9, pp. 1142–1147, Sep. 2005.

[15] L. Fan *et al.*, "Subharmonic microwave modulation stabilization of tunable photonic microwave generated by period-one nonlinear dynamics of an optically injected semiconductor laser," *J. Lightw. Technol.*, vol. 32, no. 23, pp. 4660–4666, Dec. 2014.

[16] X. Tang *et al.*, "Tbits/s physical random bit generation based on mutually coupled semiconductor laser chaotic entropy source," *Opt. Exp.*, vol. 23, no. 26, pp. 33130–33141, Dec. 2015.

[17] A.-B. Wang, Y.-C. Wang, and J.-F. Wang, "Route to broadband chaos in a chaotic laser diode subject to optical injection," *Opt. Lett.*, vol. 34, no. 8, pp. 1144–1146, Mar. 2009.
[18] X.-Z. Li, J.-P. Zhuang, S.-S. Li, J.-B. Gao, and S.-C. Chan, "Randomness evaluation for an optically injected chaotic semiconductor laser by attractor reconstruction," *Phys. Rev. E, Stat. Phys. Plasmas Fluids Relat. Interdiscip. Top.*, vol. 94, no. 4, pp. 042214-1–042214-12, Oct. 2016.
[19] A. Hurtado, A. Quirce, A. Valle, L. Pesquera, and M. J. Adams, "Nonlinear dynamics induced by parallel and orthogonal optical injection in 1550 nm vertical-cavity surface-emitting lasers (VCSELs)," *Opt. Exp.*, vol. 18, no. 9, pp. 9423–9428, Apr. 2010.
[20] F.-Y. Lin and J.-M. Liu, "Chaotic radar using nonlinear laser dynamics," *IEEE J. Quantum Electron.*, vol. 40, no. 6, pp. 815–820, Jun. 2004.
[21] J. Martin-Regalado, F. Prati, M. S. Miguel, and N. B. Abraham, "Polarization properties of vertical-cavity surface-emitting lasers," *IEEE J. Quantum Electron.*, vol. 33, no. 5, pp. 765–783, May 1997.
[22] K. Iga, "Surface-emitting laser-its birth and generation of new optoelectronics field," *IEEE J. Sel. Topics Quantum Electron.*, vol. 6, no. 6, pp. 1201–1215, Nov./Dec. 2000.
[23] F. Koyama, "Recent advances of VCSEL photonics," *J. Lightw. Technol.*, vol. 24, no. 12, pp. 4502–4513, Dec. 2006.
[24] I. Gatare, K. Panajotov, and M. Sciamanna, "Frequency-induced polarization bistability in vertical-cavity surface-emitting lasers with orthogonal optical injection," *Phys. Rev. A, Gen. Phys.*, vol. 75, no. 2, pp. 023804-1–023804-7, Feb. 2007.
[25] A. Hurtado, A. Quirce, A. Valle, L. Pesquera, and M. J. Adams, "Power and wavelength polarization bistability with very wide hysteresis cycles in a 1550 nm-VCSEL subject to orthogonal optical injection," *Opt. Exp.*, vol. 17, no. 26, pp. 23637–23642, Dec. 2009.
[26] M. S. Torre, A. Quirce, A. Valle, and L. Pesquera, "Wavelength-induced polarization bistability in 1550 nm VCSELs subject to orthogonal optical injection," *J. Opt. Soc. Amer. B, Opt. Phys.*, vol. 27, no. 12, pp. 2542–2548, Dec. 2010.
[27] A. Quirce, J. R. Cuesta, A. Valle, A. Hurtado, L. Pesquera, and M. J. Adams, "Polarization bistability induced by orthogonal optical injection in 1550-nm multimode VCSELs," *IEEE J. Sel. Topics Quantum Electron.*, vol. 18, no. 2, pp. 772–778, Mar. 2012.
[28] M. F. Salvide, C. Masoller, and M. S. Torre, "Polarization switching and hysteresis in vertical-cavity surface-emitting lasers subject to orthogonal optical injection," *IEEE J. Quantum Electron.*, vol. 50, no. 10, pp. 848–853, Oct. 2014.
[29] A. Hurtado, I. D. Henning, and M. J. Adams, "Wavelength polarization switching and bistability in a 1550-nm VCSEL subject to polarized optical injection," *IEEE Photon. Technol. Lett.*, vol. 21, no. 15, pp. 1084–1086, Aug. 1, 2009.
[30] Y. Hong, P. S. Spencer, and K. A. Shore, "Power and frequency dependence of hysteresis in optically bistable injection locked VCSELs," *Electron. Lett.*, vol. 37, no. 9, pp. 569–570, Apr. 2001.
[31] P. Guo, W. Yang, D. Parekh, C. J. Chang-Hasnain, A. Xu, and Z. Chen, "Experimental and theoretical study of wide hysteresis cycles in 1550 nm VCSELs under optical injection," *Opt. Exp.*, vol. 21, no. 3, pp. 3125–3132, Feb. 2013.
[32] A. Quirce *et al.*, "Injection locking and polarization switching in a 1550-nm VCSEL under parallel optical injection," in *Proc. 9th Reunión Española Optoelectrón. (OPTOEL)*, Jun. 2015, pp. 146–150.
[33] A. Quirce *et al.*, "Polarization switching and injection locking in vertical-cavity surface-emitting lasers subject to parallel optical injection," *Opt. Lett.*, vol. 41, no. 11, pp. 2664–2667, Jun. 2016.
[34] A. Quirce *et al.*, "Analysis of the polarization of single-mode vertical-cavity surface-emitting lasers subject to parallel optical injection," *J. Opt. Soc. Amer. B, Opt. Phys.*, vol. 34, no. 2, pp. 447–455, Feb. 2017.
[35] F. D.-L. Coarer *et al.*, "Injection locking and polarization switching bistability in a 1550 nm VCSEL subject to parallel optical injection," *IEEE J. Sel. Topics Quantum Electron.*, vol. 23, no. 6, Nov./Dec. 2017, Art. no. 1800910.
[36] F. D.-L. Coarer *et al.*, "Polarization dynamics induced by parallel optical injection in a single-mode VCSEL," *Opt. Lett.*, vol. 42, no. 11, pp. 2130–2133, Jun. 2017.
[37] G. Friart, A. Gavrielides, and T. Erneux, "Analytical stability boundaries of an injected two-polarization semiconductor laser," *Phys. Rev. E, Stat. Phys. Plasmas Fluids Relat. Interdiscip. Top.*, vol. 91, no. 4, pp. 042918-1–042918-8, Apr. 2015.
[38] D. Wang, J. Chen, G. Xia, and Z. Wu, "State bistability between pure- and mixed-mode states in a 1550 nm vertical-cavity surface-emitting laser subject to parallel optical injection," *Jpn. J. Appl. Phys.*, vol. 56, no. 7, pp. 070314-1–070314-4, Jul. 2017.
[39] M. S. Miguel, Q. Feng, and J. V. Moloney, "Light-polarization dynamics in surface-emitting semiconductor lasers," *Phys. Rev. A, Gen. Phys.*, vol. 52, no. 2, pp. 1728–1739, Aug. 1995.
[40] P. Pérez, A. Valle, and L. Pesquera, "Polarization-resolved characterization of long-wavelength vertical-cavity surface-emitting laser parameters," *J. Opt. Soc. Amer. B, Opt. Phys.*, vol. 31, no. 11, pp. 2574–2580, Nov. 2014.

DAN WANG was born in Longnan, Gansu, China, in 1994. She received the B.Sc. degree in physics from Tianshui Normal University, Tianshui, Gansu, in 2015. She is currently pursuing the M.Sc. degree in optics with Southwest University, Chongqing, China. Her research direction mainly focuses on the polarization characteristics and bistability of semiconductor lasers.

GUANG-QIONG XIA was born in Fushun, Sichuan, China, in 1970. She received the B.Sc., M.Sc., and Ph.D. degrees in optics from Sichuan University, Chengdu, Sichuan, in 1992, 1995, and 2002, respectively.

She is currently a Full Professor with the School of Physics, Southwest University, Chongqing, China. She has authored or co-authored over 140 publications including about 100 journal papers. Her current research interests include nonlinear dynamics of semiconductor lasers, synchronization and control of chaotic semiconductor lasers, chaos secure communication based on semiconductor lasers, and microwave photonics.

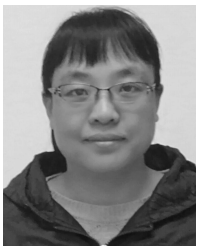

YU-SHUANG HOU was born in Tangshan, Hebei, China, in 1979. She received the M.Sc. degree in applied mathematics from Inner Mongolia University, Hohhot, China, in 2006. She is currently pursuing the Ph.D. degree in optics with Southwest University. Her current research mainly focuses on the nonlinear dynamics of semiconductor lasers and their applications.

WEN-YAN YANG was born in Chifeng, Inner Mongolia, China, in 1978. She received the M.Sc. degree in optics from Southwest University, Chongqing, China, in 2005, where she is currently pursuing the Ph.D. degree in optics. Her research direction mainly focuses on the nonlinear dynamics of semiconductor lasers.

ELUMALAI JAYAPRASATH was born in Kancheepuram, Tamilnadu, India, in 1988. He received the B.Sc. degree in physics from the Loyola College, Chennai, India, in 2008, and the M.Sc. and Ph.D. degrees in physics from Pondicherry University, Pondicherry, India, in 2010 and 2016, respectively. His thesis was on the propagation delay and synchronization of chaotic semiconductor lasers.

He is currently a Post-Doctoral Researcher with the School of Physics, Southwest University, Chongqing, China. His current research lies in the chaos synchronization of semiconductor lasers and its utilization for secure optical communications.

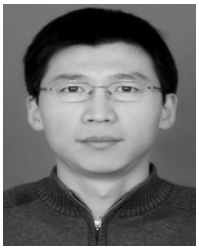

JIAN-JUN CHEN was born in Shihezi, Xinjiang, China, in 1977. He received the B.Sc. degree in physics from Xinjiang Normal University, Urumqi, Xinjiang, in 2001, and the M.Sc. and Ph.D. degrees in optics from Southwest University, Chongqing, China, in 2008 and 2017, respectively. He is currently an Associate Professor with the School of Medical Engineering and Technology, Xinjiang Medical University, Urumqi. His current research mainly focuses on the nonlinear dynamics of semiconductor lasers.

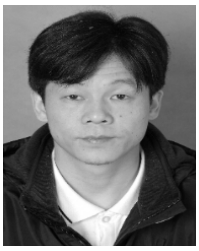

ZHENG-MAO WU was born in Wuyuan, Jiangxi, China, in 1970. He received the B.Sc., M.Sc., and Ph.D. degrees in optics from Sichuan University, Chengdu, Sichuan, China, in 1992, 1995, and 2003, respectively.

He is currently a Full Professor with the School of Physics, Southwest University, Chongqing, China. He has authored or co-authored over 100 publications. His current research interests include nonlinear dynamics of semiconductor lasers and their applications, chaotic semiconductor lasers and their applications.